

Recent Progress in High-Resolution Observations

Thomas E. Berger and Alan M. Title

*Lockheed Martin Solar and Astrophysics Laboratory, Bldg. 252,
3251 Hanover St., Palo Alto, CA 94304, USA*

Abstract. We review recent optical observations of the solar photosphere and chromosphere with an emphasis on those observations that attain spatial resolution values below $0''.25$. Results from the Dutch Open Telescope (DOT) on La Palma, the Dunn Solar Telescope (DST) on Sacramento Peak, and the Vacuum Tower Telescope (VTT) on Tenerife are reviewed. Particular emphasis is placed on results from the newly commissioned Swedish 1-meter Solar Telescope (SST) on La Palma following our successful campaigns at this instrument in 2002 and 2003. The SST with adaptive optics can now achieve $0''.1$ resolution imaging of the Sun in multiple simultaneous wavelengths. Scientific findings on the structure of sunspot penumbrae and lightbridges, small-scale magnetic elements, and faculae at the limb are reviewed. The Lockheed Solar Optical Universal Polarimeter (SOUP) birefringent tunable filter at the SST produced $0''.16$ resolution magnetograms in the summer of 2003 that have shed new light on the structure and dynamics of small-scale magnetic fields in the solar photosphere.

1. Introduction

Over the past decade progress in new telescope designs, the development of adaptive optics, and the use of advanced image processing has led to significant improvements in the spatial resolution of observations of the solar atmosphere. In particular, optical wavelength observations of the photosphere and chromosphere have improved greatly and led to new discoveries in sunspot structure and the nature of the small-scale magnetic field outside of sunspots. Here we review some of the recent results from several ground-based solar optical telescopes that have achieved the highest resolutions to date.

The definition of the term “high-resolution” is not temporally stable. As new technologies become available, what was once considered high resolution gets redefined as medium- or even low-resolution. We therefore begin by defining the current standard for high resolution observations in solar physics. We will limit our discussion to imaging and leave out considerations such as spectral resolution.

High spatial resolution is now defined by imaging of structures less than about 180 km on the Sun, or in angular terms, less than about $0''.25$. Because all features of the photosphere and chromosphere are highly dynamic at these spatial scales, it is equally important to define what constitutes high temporal resolution. Temporal resolution is defined as the minimum time between the successive images that comprise a time series or “movie.” This definition is sometimes referred to as “cadence.” The current standard for high temporal resolution is a cadence of less than 10 s. In 10 s a feature moving at the photo-

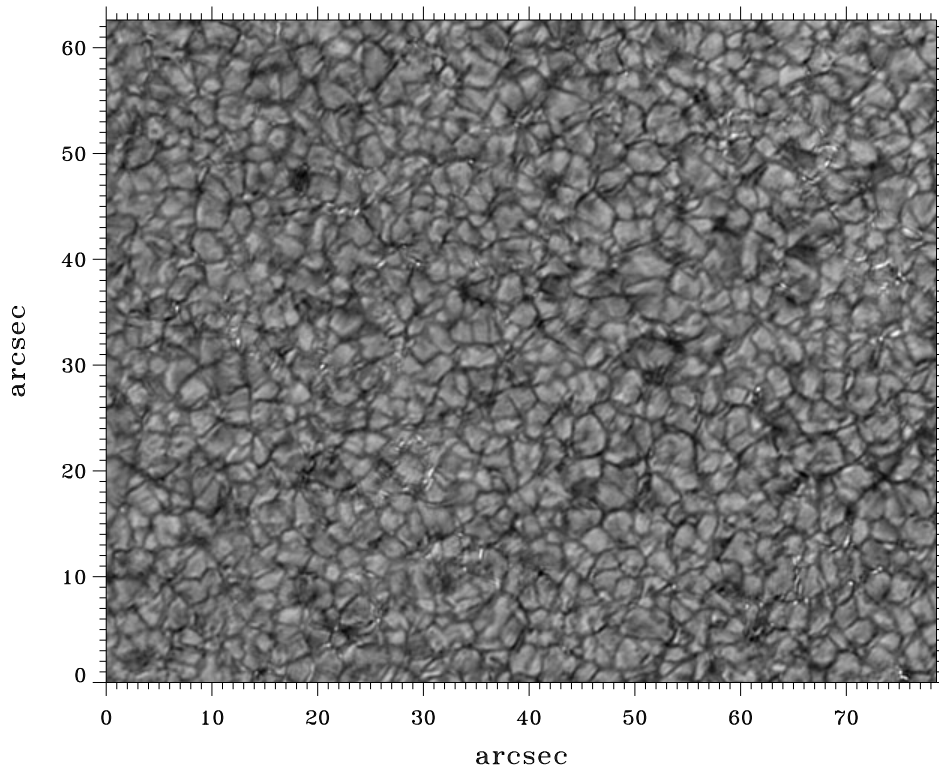


Figure 1. DOT 430.5 nm G-band image of a quiet Sun network region near disk center taken on 08-December-2002. The speckle-reconstructed image is diffraction limited ($0''.24$) across the entire FOV.

spheric sound speed of 7 km s^{-1} will travel 70 km, less than half of the maximum defined distance for high resolution imaging.

The following sections review the methods and representative results obtained over the last couple of years at some of the world's highest resolution solar telescopes.

2. The Dutch Open Telescope

The DOT[†] (Rutten et al. 2004) is a 0.45 m diameter reflecting paraboloid telescope mounted on an innovative 15 m open tower at the Roque de los Muchachos Observatory on La Palma, Spain. It was commissioned in October of 1997. The instrumentation package currently consists of several CCD cameras mounted at the parabolic prime focus, typically preceded by thin-film interference fil-

[†]<http://www.phys.uu.nl/~rutten/dot/node3.html>

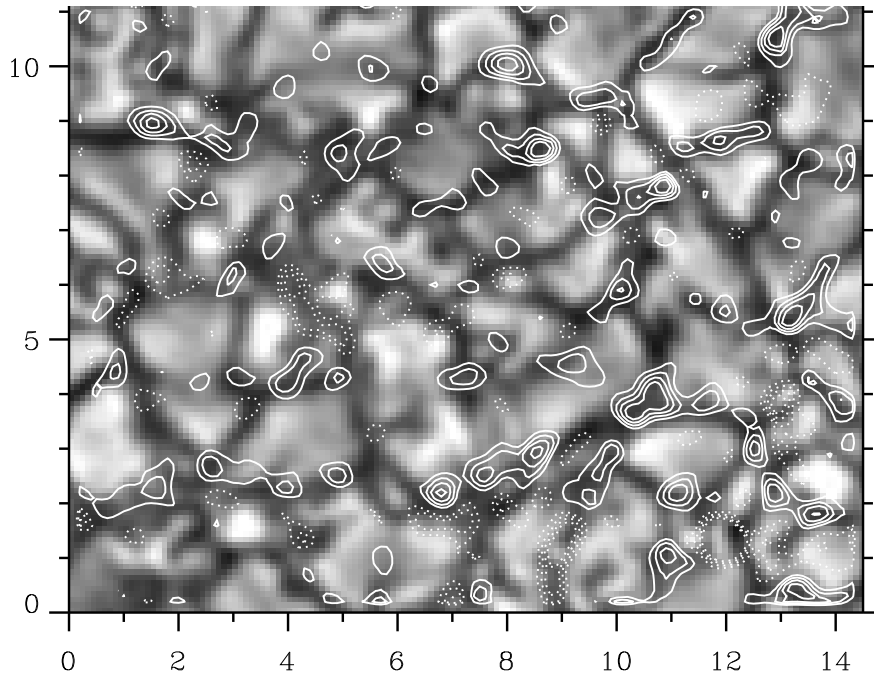


Figure 2. Fe I 630.25 nm magnetogram contours overlain on simultaneous continuum image of a quiet Sun area near disk center. Opposite polarity fields are marked by solid and dotted lines. Tickmarks are 1 arcsecond.

ters. The main innovation of the DOT is the open tower design in which the 15 m tower raises the instrument above the local boundary layer seeing and a retractable dome opens to completely expose the instrument to the ambient winds in order to flush local turbulence and instrument heat distortions away from the light beam. The diffraction limited resolution of the DOT in the G-band is $0''.24$ or about 175 km on the Sun. The temporal resolution of typical DOT time series is currently 20–30 s.

The DOT team utilizes speckle interferometric image reconstruction to achieve diffraction limited uniformity over long time series of images. Most of the science studies to date have focused on the study of solar magnetic field structure in sunspots and the quiet network primarily in the G-band 430.5 nm bandhead and the Ca II H- and K-line chromospheric lines. Figure 1 shows a 430.5 nm G-band filtergram taken on 8-December-2002. The full dataset consists of 54 min of simultaneous G-band and 396.8 nm Ca II H-line filtergrams taken at a 30 s cadence for a period of about 50 min. The resolution throughout the field-of-view (FOV) is a uniform $0''.24$ in the G-band. These data have been analyzed in a study of internetwork emission in the chromosphere by Rutten, de Wijn, & Sütterlin (2004).

3. The Vacuum Tower Telescope

The VTT, run by the Kiepenheuer-Institut für Sonnenphysik in Freiburg, Germany, is a 0.7 m vacuum tower reflector telescope at the Observatorio del Teide on the island of Tenerife, Spain. Using a combination of adaptive optics (AO) and speckle interferometric image reconstruction the VTT is capable of achieving $0''.18$ resolution in photospheric continuum (500 nm) filtergrams. Recent results include a speckle-restored Stokes-V magnetogram and simultaneous continuum sequence that achieves $0''.2$ resolution at a cadence of 30 seconds and shows an intriguing hint of ubiquitous mixed polarity kilogauss-strength magnetic flux nearly filling the intergranular lanes of a quiet Sun region near disk center (Fig. 2). The presence of mixed polarity at such strengths and scales may indicate the operation of a fast surface dynamo in the upper convection zone and photosphere. Further information on this finding can be found in Domínguez Cerdeña, Sánchez Almeida, & Kneer (2003).

4. The Dunn Solar Telescope

The DST is a 0.76 m vacuum tower reflector telescope located at the U.S. National Solar Observatory on Sacramento Peak, New Mexico, USA. An extensive AO development program at the DST (Rimmele et al. 2003) has recently resulted the telescope achieving diffraction limited imaging in good seeing conditions. The diffraction-limited resolution of the DST in the G-band 430.5 nm bandpass is $0''.14$ or about 100 km on the Sun. Figure 3 shows a G-band image of the central region of AR 10484 taken on 24-October-2003 at the DST. The image (which has not been post-processed beyond a simple telescope modulation transfer function (MTF) correction) confirms many of the new findings from the SST on penumbral filament substructure, lightbridge dark lanes, and magnetoconvective structures (see Sect. 5.1). This image was obtained using the “low-order” adaptive optics system consisting of 76 actuators; installation of a higher-order AO system consisting of 200+ actuators is in progress.

5. The Swedish 1-meter Solar Telescope

The SST (Scharmer et al. 2003a) is a 0.97 m clear aperture vacuum tower refractor telescope located at the Observatorio del Roque de los Muchachos, La Palma, Spain. This is currently the largest solar telescope with AO at a good site. It was commissioned in July of 2002. The diffraction limits of the SST in the G-band and 393.3 nm Ca II K-line are $0''.11$ and $0''.10$, respectively. Both of these limits have been achieved using the 37-element AO system (Scharmer et al. 2003b). The instrument package during the 2003 observing season consisted of three wide-band ($\sim 1\text{--}10$ Å FWHM) interference filters in front of Kodak KAF4200 and KAF1600 CCD cameras as well as the Lockheed Solar Optical Universal Polarimeter tunable birefringent narrow-band (~ 100 mÅ FWHM) filter system. The latter was used to obtain diffraction limited ($0''.16$) Fe I 630.25 nm Stokes-V magnetograms — the highest resolution magnetograms yet measured on the solar surface.

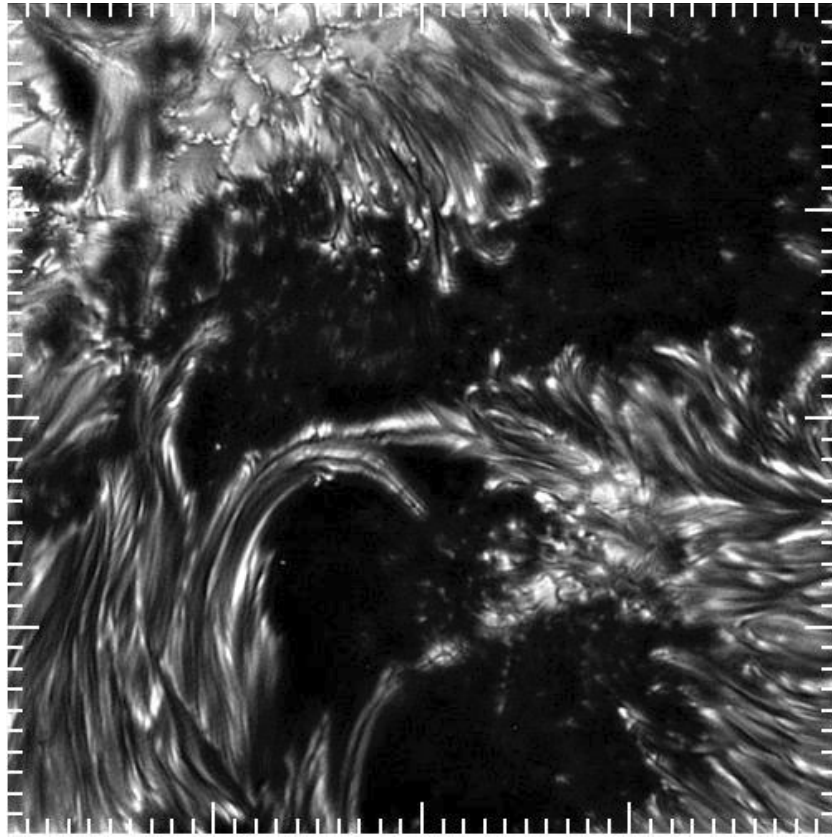


Figure 3. DST image of AR 10484 taken in the G-band on 24-October-2003. Tickmarks are arcseconds; the spatial resolution of the image is approximately 100 km.

A key factor in the achievement of diffraction limited imaging in all channels across 1 arcmin square view fields was the development of a robust post-processing code based referred to as Multi-Frame Blind Deconvolution (MFBD, Löfdahl 2002). This code is an extension of the Phase Diverse Speckle (PDS) image reconstruction code used earlier at the SST. The technique relies on the acquisition of several images in quick succession, each of which is assumed to represent a common object but with varying atmospheric blurring. Unlike PDS methods, the MFBD formulation does not require acquisition of in- and out-of focus images to recover the object information at the diffraction limit of the instrument. When used in conjunction with the AO system, MFBD has resulted in uniform quality filtergram and magnetogram time series with cadences of 10 s and lengths on the order of hours. These datasets are currently under analysis. In the following section we review some of the preliminary results from these, and earlier, SST datasets that reveal novel aspects of the solar photosphere and chromosphere.

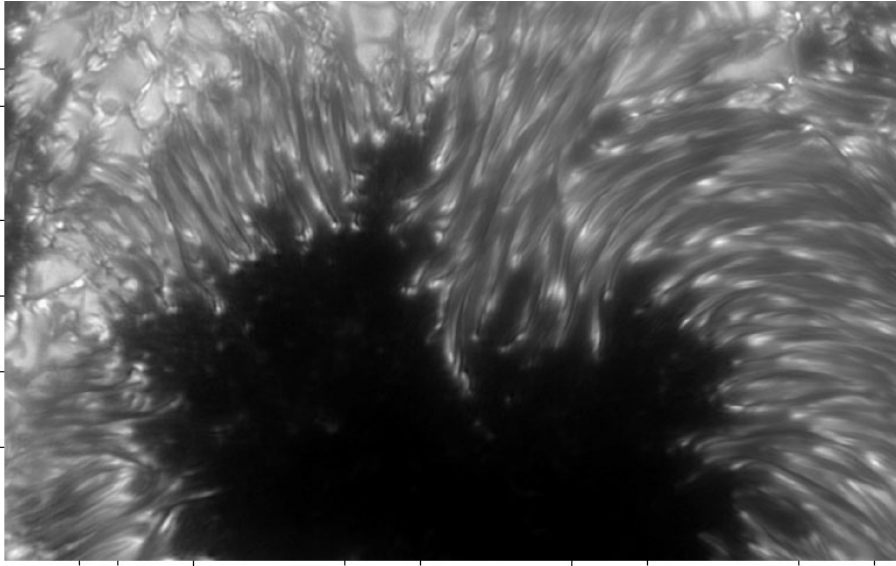


Figure 4. Detail of the penumbra/umbra boundary in a sunspot of AR 10030 imaged in the G-band on 15-July-2002. Tickmarks are 1 Mm. Note the central dark cores of approximately 100 km width in the penumbral filaments.

5.1. Sunspot Structure

Penumbral Filament Dark Cores One of the most surprising findings from the new SST is the occurrence of dark “cores” in sunspot penumbral filaments (Scharmer et al. 2002). Figure 4 shows a close up from a movie of AR 10030 taken in the G-band on 15-July-2002. It shows the central umbra/penumbra boundary of a large sunspot. Within each penumbral filament one clearly sees dark central cores that are 5–6 Mm in length and typically only 100 km or less in width. The movie shows that these cores move coherently with each penumbral filament, sometimes splitting as the filaments move. Each dark core terminates in a bright feature that also moves with the filament over time. At times, evidence of torsional waves, or “twist”, can be seen in select filament cores. There is currently no known theoretical explanation for these features. It is possible that the cores are evidence of strong vortical flows within each penumbral filament that result in the evacuation of the core interior; the brighter edges of the tubular filament are visible because of optical depth increase in the longer line of sight through the sides of the tube. Similar appearing vortices are frequently seen in terrestrial fluid flow analogs such as the vortex tubes shed by jet engine nacelles on aircraft.

Lightbridge (LB) Substructure Another discovery made using the SST was the presence of both dark central lanes and strong lateral flows in sunspot lightbridges (Berger & Berdyugina 2003). In several SST sunspot images the appearance of the dark central lane is similar: a 200–350 km wide lane that runs the length of the LB, often 6–8 Mm in length. On either side of the dark lane,

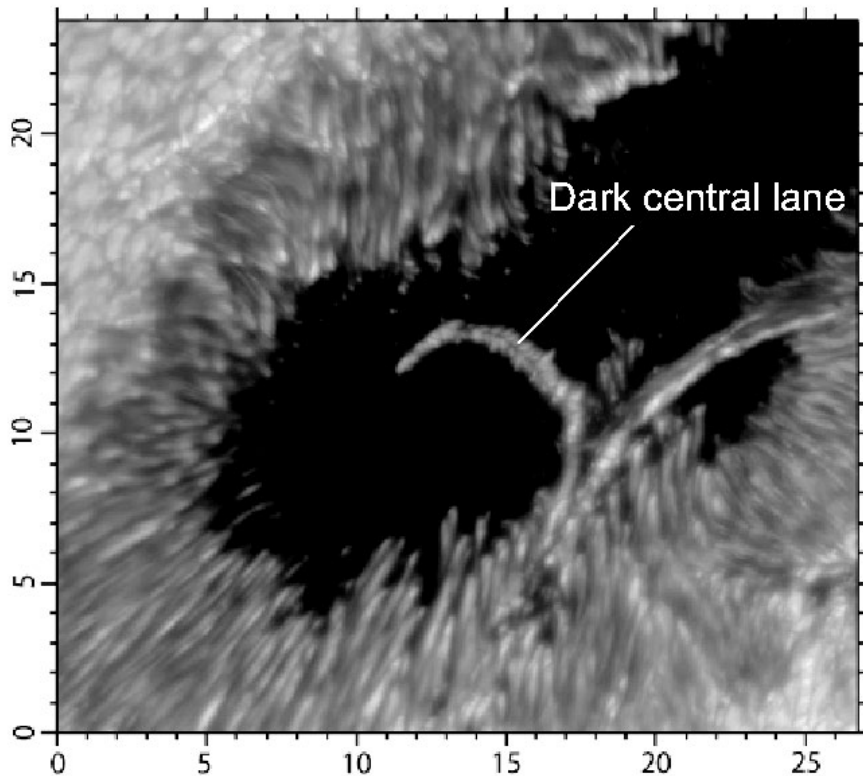


Figure 5. AR 10036 seen in the G-band on 25-July-2002 at a heliographic coordinates S7 W55 ($\mu = 0.55$). Tickmarks are 1 arcsecond. The long light-bridge shows the typical dark central lane found in many SST observations of sunspots. The lane is approximately 200 km in width and spans nearly the entire length of the bridge.

structures that appear to be coherent convective rolls are arranged generally perpendicular to the central lane. Berger & Berdyugina (2003), analyzing a time series of 705.7 nm TiO bandpass filtergrams of a long LB in the sunspot complex of AR 10132 on 25-September-2002, found that these “convective-like” structures flow along the lightbridge with an average speed of 900 m s^{-1} . In addition, the movie shows clear evidence of turning-over motions within some of the moving structures, further enhancing the evidence that these are convective rolls being transported by wave or advection flow. Hurlburt, Matthews, & Proctor (1996) have shown that a travelling wave pattern that strongly resembles the movements seen in the TiO movie is seen in their 2D MHD numerical simulations of inclined magnetic fields in convection. Relating the simulations to the LB observations implies that the inclined magnetic field lines are parallel to the LB and cause the convection to “tilt” in the direction of the inclination causing a net flow along the LB.

Figure 5 shows one particularly clear case of a dark central lane in a long LB that terminates within the umbra. Several other examples of the dark lane

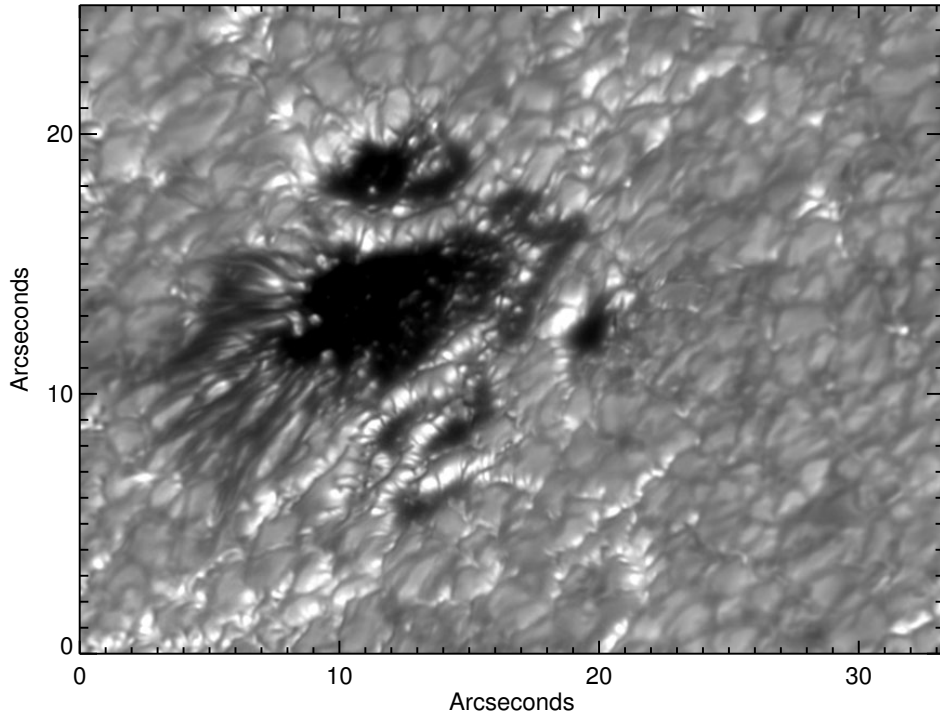


Figure 6. AR 10377 on 06-June-2003 at a disk position of about $\mu = 0.55$. Tickmarks are 1 arcsecond.

have since been found. Given its relatively large width, far above the diffraction limit of the SST and within the diffraction limit of much smaller telescopes, it is surprising that this apparently common feature of sunspot LBs has been seen only rarely in earlier observations. A few images from the predecessor to the SST, the 0.5 m Swedish Vacuum Solar Telescope (SVST), do show evidence of central lanes in LBs, but at much lower contrast. There is also a clear case shown in a sunspot drawing by Father Secchi from 1870, so this is not really a new discovery! However it is noteworthy that the increased resolution and apparently low scattering characteristics of the SST make observations of the dark central lanes a common occurrence implying that this is a typical magnetoconvective structure in sunspots.

5.2. The 3-D Photosphere

Figure 6 shows an MFB restored image of AR 10377 at a disk position of about $\mu = 0.55$ taken by Rouppe van der Voort at the SST on 6-June-2003. It is apparent that the granulation and particularly the small lightbridge across the spot are elevated above their surroundings. Preliminary measurements on another image indicates an elevation in the range of 250–400 km (Lites et al. 2004). This “3-D” appearance of the photosphere is found in all diffraction-limited SST

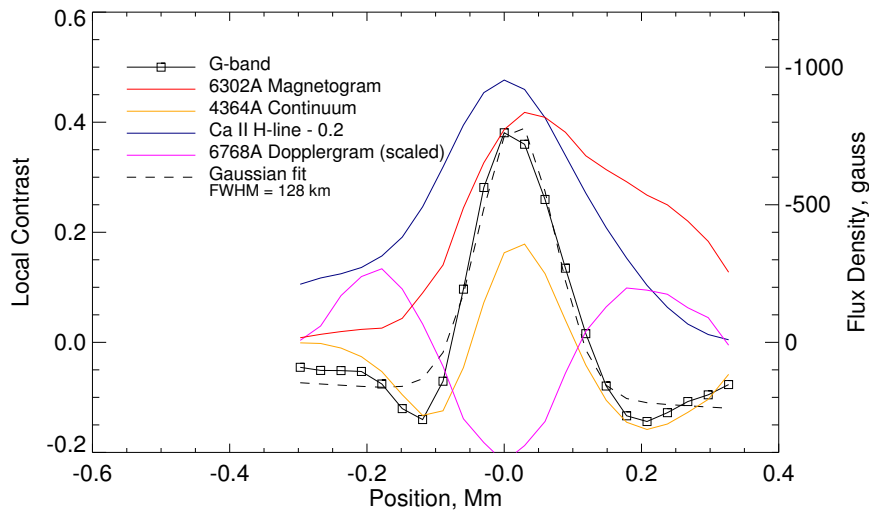


Figure 7. A cut through an isolated magnetic element in a remnant active region network near disk center on 25-May-2003. The G-band, G-band continuum, and Ca II H-line emissions are highly correlated. The magnetogram signal is wider than the G-band bright point, possibly due to the temporal smearing of the dual-image magnetogram creation algorithm. The Ni I 676.8 nm Dopplergram is not to scale but shows the existence of stronger downflows (maximum velocity approximately 540 m s^{-1}) outside of the bright point.

images taken at limbward disk positions. This particular image was used with a simultaneous Fe I 630.25 nm magnetogram to establish a 1:1 correlation between the bright “faculae” visible outside the sunspot and magnetic flux. Note that the faculae in this image appear to be extended vertically and are uniformly bright along their entire length, an appearance that is difficult to reconcile with the classical “hot-wall” model of faculae. Note also the presence of thin dark lanes across various regions near the spot. These lanes are not yet understood but may be the limbward appearance of the “canals” seen in highly magnetic regions (Scharmer et al. 2002).

5.3. Magnetic Element Structure

Finally we showcase the ability of the SST to resolve magnetic elements on the order of 100 km in diameter. Figure 7 shows a cut through an isolated magnetic element in a remnant active region network near disk center ($\mu = 0.99$) imaged on 25-May-2003. The FWHM of the G-band bright point associated with the magnetic element is 128 km. The peak measured flux density is about -1000 gauss implying that Fe I 630.25 nm magnetogram may be close to resolving the structure as well (assuming that the typical magnetic element field strength is about 1200–1500 gauss). The calibration of the SOUP magnetogram

is based on comparison to cotermporal MDI magnetograms and thus is uncertain to within about a factor of 2 making the issue of magnetic field resolution difficult to quantify. The Ni I 676.8 nm Dopplergram shows that there are downflows surrounding the magnetic element (on the order of several hundred m s^{-1} ; not scaled on the plot), but within the element itself the downflow velocity is significantly reduced.

6. Conclusion

The advent of novel telescope designs, adaptive optics, and sophisticated image post-processing techniques has recently led to significant progress in high-resolution solar physics. The term high-resolution has been effectively redefined to encompass spatial scales below about $0''.25$ and temporal scales on the order of 10 s. At these new levels of resolution many new phenomena, particularly in the structure and sub-structure of the photospheric magnetic field and its effect on convection, have been discovered.

The Solar-B FPP instrument will revolutionize the high-resolution solar optical imaging field with its $0''.2$ resolution and continuous, seeing-free, generation of multi-wavelength filtergrams, magnetograms, and Dopplergrams. Maximum utilization of this capability will depend on developing more sophisticated methods of data exploration and analysis in order to handle the high volumes of very large format imagery being generated by Solar-B. With these new tools, it is certain that a myriad of discoveries will be made in sunspot structure, magnetic field generation and evolution, and the links between photospheric magnetic fields and the heating of the solar outer atmosphere.

References

- Berger, T. E., & Berdyugina, S. V. 2003, *ApJ*, 589, L117
- Domínguez Cerdeña, I., Sánchez Almeida, J., & Kneer, F. 2003, *A&A*, 407, 741
- Hurlburt, N. E., Matthews, P. C., & Proctor, M. R. E. 1996, *ApJ*, 457, 933
- Löfdahl, M. G. 2002, in *Proc. SPIE*, Vol. 4792, *Image Reconstruction from Incomplete Data II.*, ed. P. J. Bones, M. A. Fiddy, & R. P. Millane, 146
- Lites, B. W., Scharmer, G. B., Berger, T. E., & Title, A. M. 2004, *Solar Phys.*, 221, 65
- Rimmele, T., & 10 co-authors 2003, in *Proc. SPIE*, Vol. 4839, *Adaptive Optical System Technologies II.*, ed. P. L. Wizinowich & D. Bonaccini, 635
- Rutten, R. J., de Wijn, A. G., & Sütterlin, P. 2004, *A&A*, 416, 333
- Rutten, R. J., Hammerschlag, R. H., Bettonvil, F. C. M., Sütterlin, P., & de Wijn, A. G. 2004, *A&A*, 413, 1183
- Scharmer, G. B., Bjelksjo, K., Kohonen, T. K., Lindberg, B., & Petterson, B. 2003a, in *Proc. SPIE*, Vol. 4853, *Innovative Telescopes and Instrumentation for Solar Astrophysics*, ed. S. L. Keil, S. V. Avakyan, & S. I. Vavilov, 341
- Scharmer, G. B., Dettori, P. M., Löfdahl, M. G., & Shand, M. 2003b, in *Proc. SPIE*, Vol. 4853, *Innovative Telescopes and Instrumentation for Solar Astrophysics*, ed. S. Keil & S. V. Avakyan, 370
- Scharmer, G. B., Gudiksen, B. V., Kiselman, D., Löfdahl, M. G., & Rouppe van der Voort, L. H. M. 2002, *Nat*, 420, 151